# Features of the holes formation by counterboring tool

**I P Deryabin and V G Shalamov**

South Ural State University, 76 Lenin prospect, Chelyabinsk, Russia

E-mail: deryabinip@susu.ru

**Abstract**. The article discusses the process of shaping holes with three-bladed counterboring tools, taking into account the inaccuracies of sharpening the cutting part and feed fluctuations arising due to axial beats of the machine spindle. The shaping schemes have been constructed, equations have been derived for calculating the areas of cut-off allowance sections for which the radial cutting forces are calculated. A comparison obtained by mathematical dependencies and in the scale model in a three-dimensional modeling system for the values of the cut section areas was made. Vector sum of radial cutting forces allows to determine the point's coordinates of the resulting surface, which can determine the parameters of machining accuracy.

## 1. Mathematical models of hole shaping by counterboring tool

When developing mathematical models of hole shaping by counterboring tool, it is necessary to take into account the following factors that lead to changes in the areas of cut off stock sections: fluctuations in the tool feed due to axial beating of the machine spindle; inaccuracies of cutting tool geometry arising during sharpening, etc. In existing models [1, 3-5], the cut-off stock section is taken as a simple parallelogram because the real metering of countersink cutting blades is not considered within the sharpening of the entering angle. However, studies carried out taking into account the real dissymmetry of the cutting part of the counterboring tool [2, 6-8], namely, the inaccuracies of sharpening the entering angle – φ and the axial lagging of the cutting blade's tops, showed a significant influence of these factors on the accuracy of multi-hole machining [9,10].

Therefore, it is necessary to take into account the difference between the entering angles in the schemes and models of shaping. The following combinations of the entering angle φ of different tool blades are possible:

1) $\varphi1>\varphi2>\varphi3$ 2) $\varphi1<\varphi2<\varphi3$ 3) $\varphi1<\varphi2>\varphi3$,

where φ1, φ2 and φ3 are the entering angles of the first, second and third blades respectively.

The cut sections of the allowance for each blade will be distributed as follows (figure 1).

The diagrams show the sequence of the cut-off stock of the tool blade through 120 degrees and the position of the radius vectors of the cutting blade vertices ρ(φ).

The above schemes are constructed without taking into account the axial runout of the spindle, leading to feed fluctuations with the adopted frequency of oscillations per full spindle revolution. In this case, it is obvious that with a variable feed, the value of the cut-off stock section will also be variable. To estimate the range of the intermittent feed, we calculate the feed rate Sp using the equation (1) at three different angles of rotation 120 °, 240 °, 360 °. We carry out the construction for each of the variants of the angle combinations (figure 2).

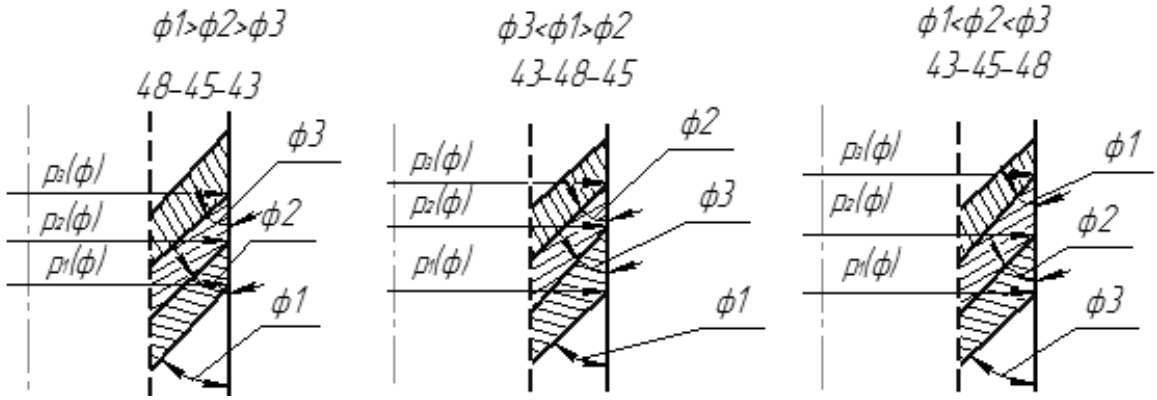


**Figure 1.** Cut off cross-sections of stock by counterboring tool blades with different combinations of entering angles.

$$S_{\Pi} = \frac{S + \Delta S \cdot \cos\psi}{3}, \quad (1)$$

where S – nominal feed rate,

ΔS – feed amplitude.

To develop mathematical models, it is necessary to compile the power balance equations (vector sum) of the thrust force. Values of the thrust force will be taken proportional to the areas of the cut sections with the corresponding coefficients of proportionality, which we call cutting coefficients.

The area of the cut sections can be determined by shaping schemes. The area of the cut stock with one tooth of the tool F (figure 3) will be equal to the value, which is defined as the total area of two irregular triangles obtained after holding the smaller of the diagonals in the obtuse-angled trapezium, such is the figure obtained in the cross section of the removed stock. The calculation is based on the formulas of geometry and the properties of angles. The result of the calculation was the formula (2) which is a mathematical model for calculating the cross-sectional area according to specified parameters, such as the main angles in the plan, the size of the stock and the feed.

$$F = \left( \frac{S}{3} \cdot \frac{\rho \cdot \sin(\frac{\pi}{2})}{\sin\left(\left(\frac{\zeta}{2} - \varphi 1 \cdot \frac{180}{\pi}\right) \cdot \frac{\pi}{180}\right)} \cdot \frac{\sin\left(\left(\frac{\zeta}{2} - \varphi 1 \cdot \frac{180}{\pi}\right) \cdot \frac{\pi}{180}\right)}{2} \right) + \cdot$$

$$\left( \frac{\rho \cdot \sin\left(\frac{\pi}{2}\right)}{2\sin\left(\left(\frac{\zeta}{2} - \varphi 1 \cdot \frac{180}{\pi}\right) \cdot \frac{\pi}{180}\right)} \cdot \sqrt{\left(\frac{S}{3}\right)^2 + \left( \frac{\rho \cdot \sin(\frac{\pi}{2})}{\sin\left(\left(\frac{\zeta}{2} - \varphi 1 \cdot \frac{180}{\pi}\right) \cdot \frac{\pi}{180}\right)} \right)^2 - 2 \cdot \frac{S}{3} \cdot \frac{\rho \cdot \sin(\frac{\pi}{2})}{\sin\left(\left(\frac{\zeta}{2} - \varphi 1 \cdot \frac{180}{\pi}\right) \cdot \frac{\pi}{180}\right)}} \right)$$

$$\sqrt{\cos\left(\left(\frac{\zeta}{2} - \varphi 1 \cdot \frac{180}{\pi}\right) \cdot \frac{\pi}{180}\right)} \cdot \sin\beta 3 \quad (2)$$

The accuracy of the calculation is verified by constructing shaping schemes in the Compass 3D V13 three-dimensional modeling system, a scale model.

Table 1 shows the comparison results of the cut section's areas obtained in the mathematical and scale models.

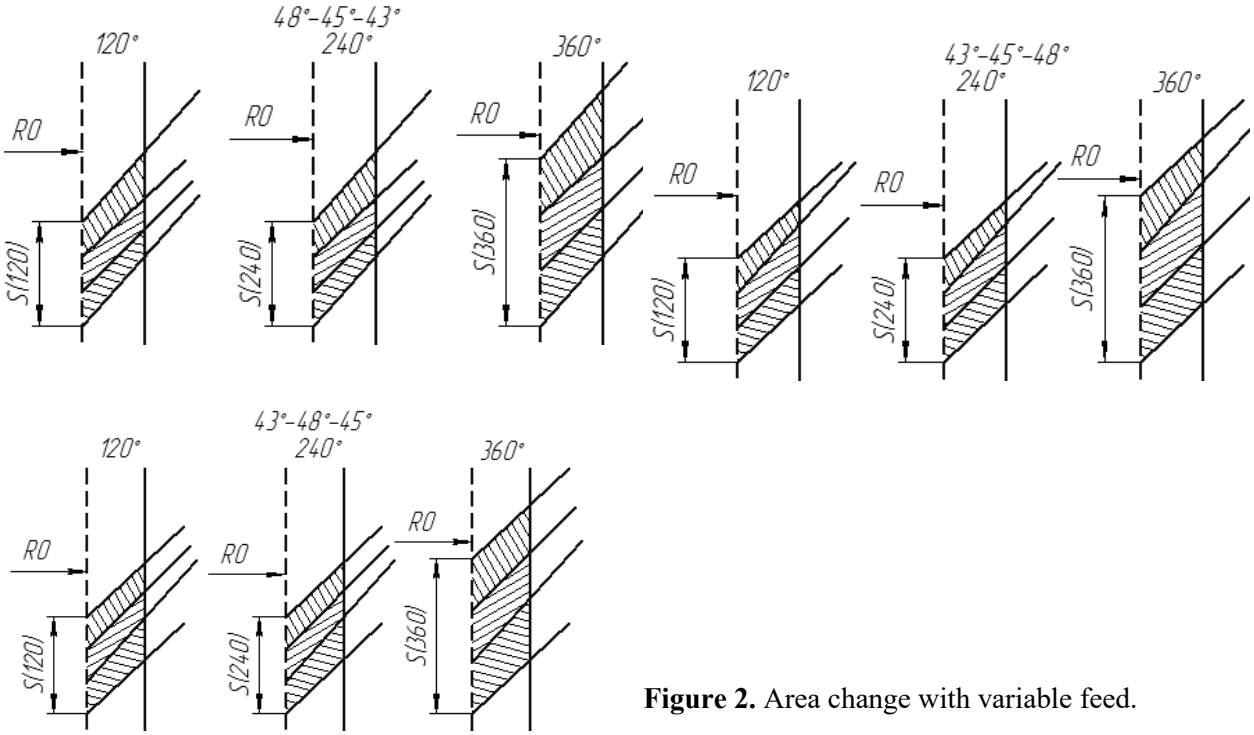


**Figure 2.** Area change with variable feed.

To estimate the change in the area of the material being cut by each of the blades, we plotted the dependences on the angle of tool rotation. In Figure 4 we can see the extreme values of both the areas and the feed fluctuations as a result of axial spindle beats.

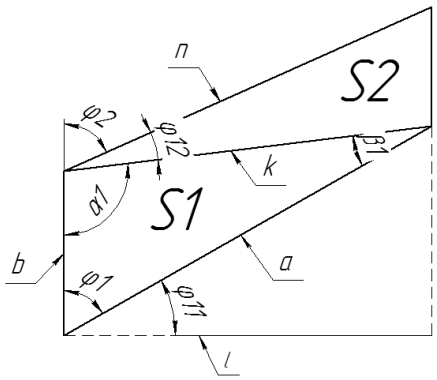


**Figure 3.** The area of the cut layer.

**Table 1.** Checking the calculation equation graphically.

| Entering angle φ1, φ2. | Feed per tooth S/3 | The amount of stock on the side | Calculate F according to the equation (2) | Measurement in Compass 3D V13 | Measurement inaccuracy δ (%) |
|---|---|---|---|---|---|
| 45,47 | 0,5 | 1 | 0,466 | 0,4662 | 0,043 |
| 45,47 | 0,3 | 1 | 0,2663 | 0,2662 | 0,038 |
| 45,47 | 0,5 | 1,3 | 0,593 | 0,5929 | 0,017 |
| 47,43 | 0,5 | 2 | 1,279 | 1,279 | - |
| 47,43 | 0,5 | 1,6 | 0,979 | 0,979 | - |
| 47,43 | 0,4 | 2 | 1,0797 | 1,0797 | - |

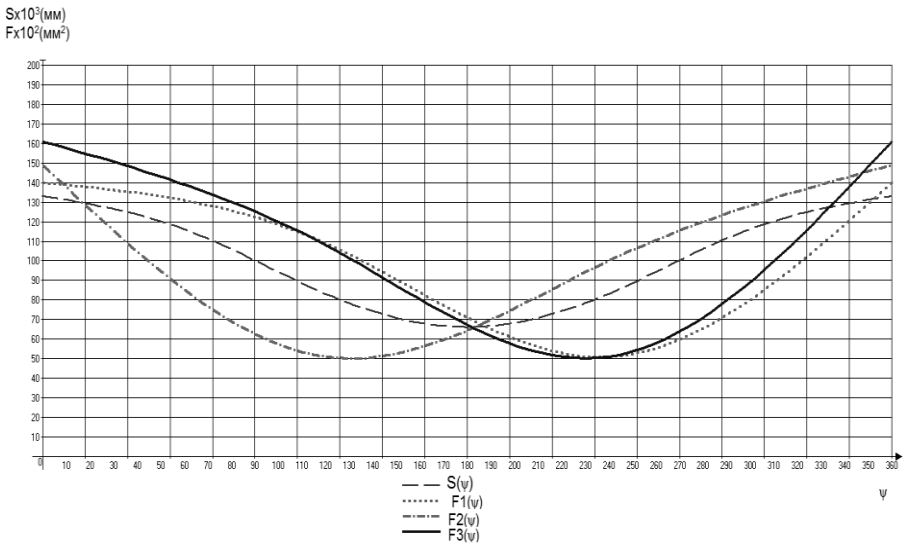


**Figure 4.** Dependence of areas and feed on the angle of counterboring tool rotation.

According to the mathematical model of shaping, we determine the force vectors P1, P2, P3. Using the rule of geometric addition of vectors, we add the force vectors of each blade P1, P2, P3. (Figure 5). The end of the total vector PΣ will determine the position of the tool axis every 10 °, i.e. the position of the tool is determined in each of the 36 (360 ° / 10 °) positions during one rotation.

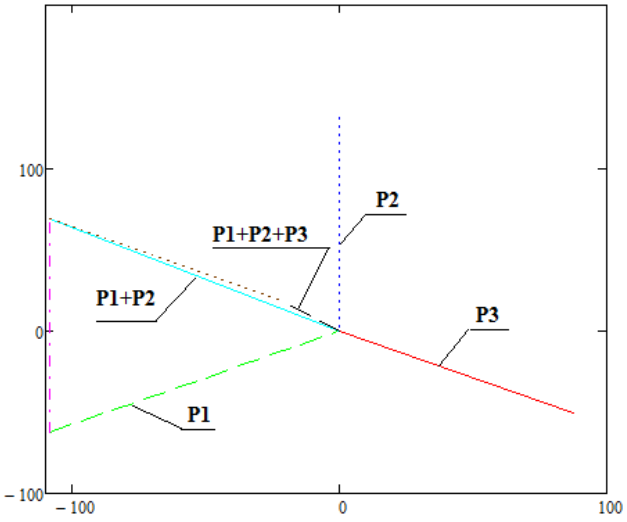


**Figure 5.** Example of sum vector addition.

From the ends of the sum vectors P∑, we draw circles corresponding to the counterboring tool diameter, for example, d = 10 mm. We also build radius vectors from the ends of the sum vectors, the ends of which will lie on the circles corresponding to the counterboring tool diameter. The obtained coordinates (Figure 6) allow us to determine the parameters of hole accuracy. To do this, we use the method of searching through every 3 points for construct circles and find the one inscribed with the largest radius, which will characterize the specified section of the hole.

For clarity, the position of the points relative to the main circle (not lying on it) is placed at a 20-fold distance from it (Figure 6).

The obtained surface coordinates of the hole allow us to calculate the processing accuracy parameters: diametral size, shape and location of the axis.

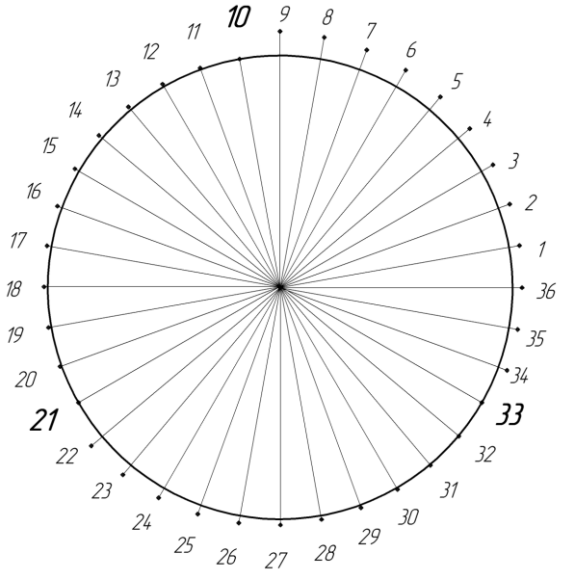


**Figure 6.** The coordinates of the hole surface.

**References**

[1] Deryabin I P 2005 *Izvestiya Chelyabinskogo nauchnogo tsentra* **2(28)** 42-7
[2] Deryabin I P 2012 Tekhnologiya mashinostroeniya **6** 12-5
[3] Fernández-Pérez J, Cantero J L, Díaz-Álvarez J and Miguélez M H 2017 *Composite Structures* **178** 157-61
[4] Cheng H, Zhang K, Wang N, Luo B and Meng Q 2017 *International Journal of Advanced Manufacturing Technology* **89(5-8)** 2063-76
[5] Wang J H and Wang M R 2016 *Optics Communications* ***371*** 206-12
[6] Dong H, Tang X, He F and Liu S 2016 *Hangkong Xuebao/Acta Aeronautica et Astronautica Sinica* **37(11)** 3554-62
[7] Ramzi R and Bakar E A 2018 *IOP Conference Series: Materials Science and Engineering* **370(1)** 012041
[8] Ma X et al. 2018 *International Journal of Advanced Manufacturing Technology* **95(1-4)** 785-95
[9] Bi Y-B, Xu C, Fan X-T and Yan W-M 2017 *Journal of Zhejiang University (Engineering Science)* **51(2)** 312-8
[10] Jallouli I, Mosbah H and Krichen A 2017 *Mechanika* **23(3)** 473-8